# Multimeric Complexes among Ankyrin-Repeat and SOCS-box Protein 9 (ASB9), ElonginBC, and Cullin 5: Insights into the Structure and Assembly of ECS-type Cullin-RING E3 Ubiquitin Ligases

Jemima C. Thomas, Dijana Matak-Vinkovic, Inge Van Molle, and Alessio Ciulli*,[†]

Department of Chemistry, University of Cambridge, Lensfield Road, Cambridge CB2 1EW, United Kingdom

S *Supporting Information*
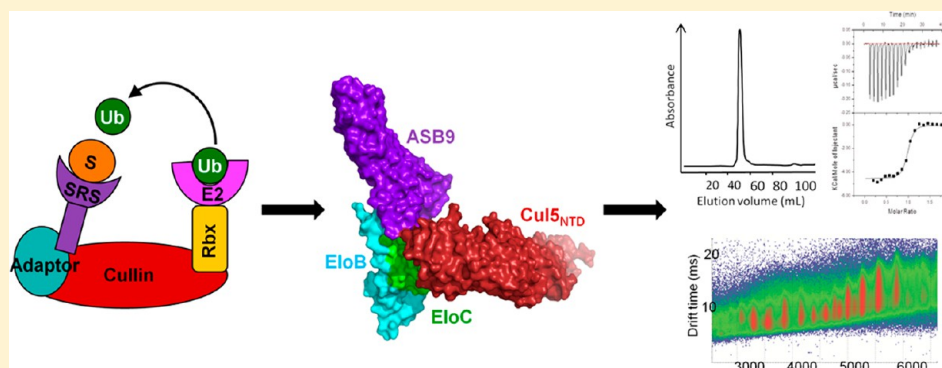
ABSTRACT: Proteins of the ankyrin-repeat and SOCS-box (ASB) family act as the substrate-recognition subunits of ECS-type (ElonginBC−Cullin−SOCS-box) Cullin RING E3 ubiquitin ligase (CRL) complexes that catalyze the specific polyubiquitination of cellular proteins to target them for degradation by the proteasome. Therefore, ASB multimeric complexes are involved in numerous cell processes and pathways; however, their interactions, assembly, and biological roles remain poorly understood. To enhance our understanding of ASB CRL systems, we investigated the structure, affinity, and assembly of the quaternary multisubunit complex formed by ASB9, Elongin B, Elongin C (EloBC), and Cullin 5. Here, we describe the application of several biophysical techniques including differential scanning fluorimetry, isothermal titration calorimetry (ITC), nanoelectrospray ionization, and ion-mobility mass spectrometry (IM−MS) to provide structural and thermodynamic information for a quaternary ASB CRL complex. We find that ASB9 is unstable alone but forms a stable ternary complex with EloBC that binds with high affinity to the Cullin 5 N-terminal domain (Cul5$_{NTD}$) but not to Cul2$_{NTD}$. The structure of the monomeric ASB9−EloBC−Cul5$_{NTD}$ quaternary complex is revealed by molecular modeling and is consistent with IM−MS and temperature-dependent ITC data. This is the first experimental study to validate structural information for the assembly of the quaternary N-terminal region of an ASB CRL complex. The results suggest that ASB E3 ligase complexes function and assemble in an analogous manner to that of other CRL systems and provide a platform for further molecular investigation of this important protein family. The data reported here will also be of use for the future development of chemical probes to examine the biological function and modulation of other ECS-type CRL systems.

The E1 (activating), E2 (conjugating), and E3 (ligating) ubiquitination cascade plays a key role in controlling cellular protein levels by catalyzing the polyubiquitination of substrate proteins, leading to their subsequent proteasomal degradation.[1−3] The E3 ubiquitin ligases impart specificity for this process and act by bringing a ubiquitin-loaded E2 enzyme and the substrate into close proximity to allow the ubiquitin transfer to occur.[4] The Cullin-RING ligases (CRLs) function as multisubunit protein complexes (Figure 1A). They are the largest family of E3 ligases in eukaryotes, consisting of ~400 members[5] that target ~20% of the proteins degraded by the proteasome.[6] CRLs are therefore involved in a myriad of cellular processes, including cell-cycle control, gene transcription, and signal transduction,[7] so it is of great interest to study how these complex molecular machines assemble and function.

Cullin (Cul) proteins are composed of two domains. The N-terminal domain consists of three repeats of five α-helix bundles (Figure 1B) and binds to a substrate recognition subunit (SRS), usually via adaptor proteins, whereas the C-terminal domain binds to RING-box proteins (Rbx) to recruit the ubiquitin-loaded E2 enzyme (Figure 1A).[8] Therefore, Cullin acts as a scaffold on which to build the modular CRL functional complexes. There are seven Cullin proteins in the human genome (Cul1, Cul2, Cul3, Cul4a, Cul4b, Cul5, and Cul7),[7,9]
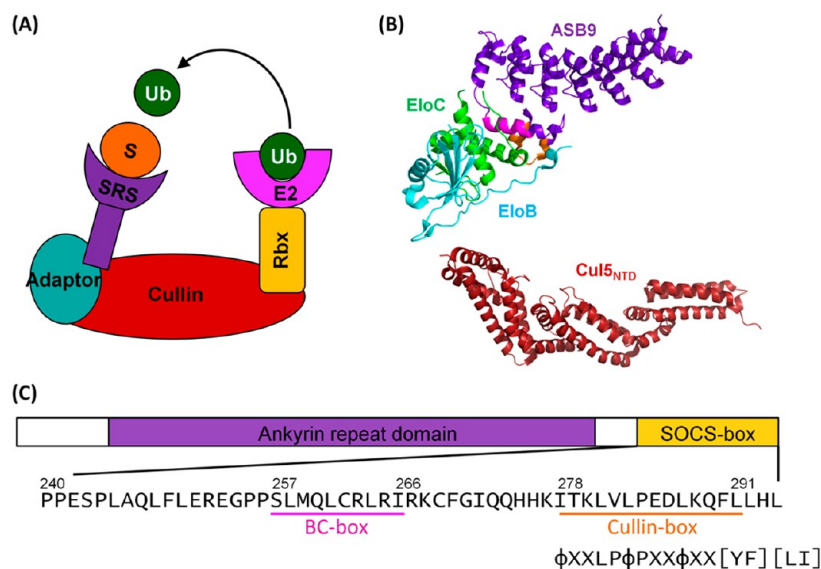
Figure 1. ASB9 is part of a Cullin-RING E3 ubiquitin ligase complex. (A) Cartoon showing the assembly of Cullin-RING E3 ubiquitin ligases. ASB9 acts as a substrate recognition subunit (SRS) utilizing Elongin B and Elongin C as adaptor proteins to bind the Cullin N-terminal domain. The Cullin C-terminal domain binds RING-box protein (Rbx) to bring the ubiquitin (Ub)-loaded E2 enzyme into close proximity with substrate (S), allowing polyubiquitination to occur. (B) Crystal structures of the ASB9−EloBC ternary complex (PDB 3ZKJ) and Cullin 5 N-terminal domain (Cul5$_{NTD}$, PDB 2WZK). ASB9 is shown in purple, EloC, in green, and EloB, in cyan. The ASB9 BC-box is shown in pink and the Cullin-box in orange. Cul5$_{NTD}$ is shown in red. (C) Sequence schematic of ASB9 highlighting the C-terminal SOCS-box domain. The EloBC-binding region (BC-box) is underlined in pink, and the Cullin 5-binding box underlined in orange. The canonical Cullin 5-binding motif is shown underneath and is also underlined in orange (φ is a hydrophobic residue and X is any residue).

and each one binds to specific adaptor proteins and motifs within the SRS. Cul1 binds F-box proteins via the adaptor Skp1,[10] Cul4 recruits WD40-containing proteins via linker-damaged DNA binding protein (DDB1),[5] and Cul3 is unusual in that it recruits the adaptor and SRS in the same Bric-a-Brac, Tramtrack, and Broad complex (BTB)-domain proteins.[11] In contrast, Cul2 and Cul5 both use Elongin B and Elongin C as adaptor proteins to bind VHL-box[12] and SOCS-box proteins,[13] respectively, as part of ECS-type (EloBC−Cullin−SOCS-box) CRLs. CRL ligase activities are controlled by several complex regulation mechanisms, including activation by conjugation with the protein NEDD8 (neural precursor cell expressed, developmentally downregulated 8) and inhibition by binding of CAND1 (cullin-associated and neddylation-dissociated 1).[14] Interestingly, it is emerging that many CRLs may function as dimers as well as or instead of as monomeric multisubunit complexes.[15−17] CRL dimerization interactions tend to occur through the adaptor proteins or SRS, for example, BTB^{SPOP}−Cul3,[18] BTB^{KLHL11}−Cul3,[19] and Fbx4−Skp1.[20]

The ankyrin-repeat and SOCS-box (ASB) proteins are postulated to act as substrate-recognition domains in ECS-type CRL complexes.[21−24] However, this protein family is currently poorly understood, and there is limited knowledge of their degradation substrates and cellular roles. Crucially, no studies to date have investigated the assembly of ASB E3 ligase component structures or their interaction affinities. Here, we provide a biophysical and structural characterization of the noncovalent complex formed between ankyrin-repeat and SOCS-box protein 9 (ASB9), Elongin B (EloB), Elongin C (EloC), and Cul5. ASB9 (Figure 1B,C) has previously been shown to act as the substrate-recognition domain of an E3 ligase that includes EloB, EloC, Cul5, and Rbx2.[25] ASB9 is predominantly expressed in the kidney and testes, and it has been shown to bind to and ubiquitinate brain-type cytosolic

creatine kinase B[25] and ubiquitous mitochondrial creatine kinase.[26] However, the exact function of ASB9 remains unknown. Recent evidence suggests that ASB9 could be a biomarker for human breast cancer,[27] and it has also been linked to colorectal cancer,[28] suggesting that it may be a new potential drug target against these diseases. In this Article, we show that ASB9 forms a high-affinity 1:1:1:1 quaternary complex with EloB, EloC, and Cul5, and we describe a structural model for this complex that is consistent with ion-mobility mass spectrometry and temperature-dependent ITC data. These results present insights into the assembly of ECS-type CRLs and provide a platform for further investigation of the ASB protein family.

■ EXPERIMENTAL PROCEDURES

Protein Expression and Purification. Recombinant human ASB9 (residues 35−294), Elongin B (residues 1−118), and Elongin C (residues 17−112) were coexpressed in *Escherichia coli* BL21(DE3) cells. Coexpression of the ASB9−EloBC complex was achieved by cotransforming a pNIC plasmid containing the ASB9 coding sequence with a C-terminal TEV cleavage site followed by His$_6$ and FLAG tags (a gift from Dr. Alex Bullock, Structural Genomics Consortium, University of Oxford) along with a pCDF_Duet plasmid containing the Elongin B (TCEB2) and Elongin C (TCEB1) coding sequences as a bicistronic message (a gift from Dr. Yong Xiong, Yale University). A single colony from the transformation was used to grow a starter culture in 100 mL of Luria−Bertani (LB) media containing 50 μg/mL of kanamycin and 50 μg/mL of streptomycin at 37 °C for 18 h. Ten milliliters of the starter culture was added to 1 L of LB media supplemented with 50 μg/mL of kanamycin and 50 μg/mL of streptomycin, and the cells were grown at 37 °C until the OD$_{600}$ reached ∼0.5, at which point protein expression was

induced with 0.1 mM isopropyl-1-thio-β-D-galactopyranoside for 18 h at 18 °C.

The recombinant human Cullin 5 N-terminal domain (Cul5$_{NTD}$, residues 1−386 with solubilizing mutations V341R and L345D) was also expressed in *E. coli* BL21(DE3) cells from a pNIC plasmid containing the CUL5 coding sequence with C-terminal His$_6$ and FLAG tags and a TEV cleavage site (a gift from Dr. Alex Bullock). A single colony from the transformation was used to grow a starter culture in 100 mL of LB media supplemented with 50 μg/mL of kanamycin at 37 °C for 18 h. Five milliliters of the starter culture was added to 1 L of LB media containing 50 μg/mL of kanamycin, the cells were grown to an OD$_{600}$ of ∼0.5, and protein expression was induced with 0.5 mM isopropyl-1-thio-β-D-galactopyranoside for 18 h at 18 °C.

The recombinant human Cullin 2 N-terminal domain (Cul2$_{NTD}$, residues 8−384 with solubilizing mutations V340R and L344D) was expressed in *E. coli* Rosetta cells from a pNIC plasmid containing the CUL2 coding sequence followed by C-terminal His$_6$ and FLAG tags and a TEV cleavage site (a gift from Dr. Alex Bullock). A single colony from the transformation was used to grow a starter culture in 100 mL of LB media containing 50 μg/mL of kanamycin and 30 μg/mL of chloramphenicol at 37 °C for 18 h. Twenty milliliters of the starter culture was added to 1 L of LB media containing 50 μg/mL of kanamycin and 30 μg/mL of chloramphenicol, the cells were grown to an OD$_{600}$ of ∼0.8, and protein expression was induced with 0.5 mM isopropyl-1-thio-β-D-galactopyranoside for 18 h at 18 °C.

ASB9−EloBC, Cul5$_{NTD}$, and Cul2$_{NTD}$ were independently purified using the following procedure. The cell pellets were harvested by centrifugation at 4000 rpm (4 °C) for 20 min and resuspended in 20 mL of lysis buffer containing 50 mM HEPES, pH 7.5, 500 mM NaCl, 5% glycerol, 5 mM imidazole, and 1× EDTA-free protease-inhibitor tablet (Roche) for lysis using a french press. The cell lysate was filtered through a 0.45 μm syringe filter and purified by passing it through 3 mL of Ni-NTA beads (GE Healthcare). The beads were washed three times with wash buffer (50 mM HEPES, pH 7.5, 500 mM NaCl, 5% glycerol, and 30 mM imidazole), and the protein was eluted using 5 mL of each elution buffer (50 mM HEPES, pH 7.5, 500 mM NaCl, and 5% glycerol containing 50, 100, 150, and 250 mM imidazole). The elution fractions were pooled, and the His$_6$ and FLAG tags were cleaved by incubation of the protein with TEV (1:75 TEV/protein) at 4 °C for 18 h. The protein solution was diluted with 50 mM HEPES, pH 7.5, 500 mM NaCl, and 5% glycerol to dilute the imidazole followed by a second Ni-NTA affinity purification, and the flow through was collected. The flow through was further purified by preparative size-exclusion chromatography using a Superdex 75 16/60 column (GE Healthcare) with a running buffer consisting of 50 mM HEPES, 100 mM NaCl, pH 7.5, and 1 mM TCEP. (The yields of the purifed products were ASB9−EloBC ∼10 mg/L, Cul5$_{NTD}$ ∼40 mg/L, and Cul2$_{NTD}$ ∼8 mg/L.) See Figure S1 for SDS-PAGE analysis of Cul2$_{NTD}$.

Reconstitution of the ASB9−EloBC−Cul5$_{NTD}$ Quaternary Complex. Equimolar amounts of cleaved and purified ASB9−EloBC (430 μM) and Cul5$_{NTD}$ (470 μM) were mixed and incubated at room temperature for 20 min before purification by preparative size-exclusion chromatography using a Superdex 75 16/60 column (GE Healthcare) equilibrated in 50 mM HEPES, 100 mM NaCl, pH 7.5, and 10 mM DTT.

Native Nanoelectrospray Ionization Mass Spectrometry (nanoESI−MS). NanoESI−MS measurements were performed in positive ion mode using a Synapt HDMS quadrupole ion-trap IM−MS instrument described in detail previously (Waters, U.K.).[29,30] The samples were prepared by a buffer exchange of the protein into 500 mM ammonium acetate, pH 7.0, using micro Biospin columns (Bio-Rad, U.K.). To preserve the noncovalent interactions, the typical instrument settings were as follows: capillary voltage, 1.7 kV; sample-cone and extraction-cone voltages, 80 and 1.4 V, respectively; trap, 12 V; transfer, 13 V; backing pressure, 3.8 mbar; trap pressure, 5×10^{-2} mbar; time-of-flight analyzer pressure, 1.17×10^{-6} mbar. All spectra were calibrated internally using a solution of cesium iodide (100 mg/mL). The data were processed with MassLynx 4.0 software (Waters/Micromass).

Ion-Mobility Mass Spectrometry (IM−MS). IM−MS measurements for the ASB9−EloBC−Cul5$_{NTD}$ protein complex were performed with the Synapt HDMS. N$_2$ gas was used in the ion-mobility cell at 0.5 mbar pressure, whereas the traveling wave velocity was 250 ms^{-1}. To optimize the IM separation for the ASB9−EloBC−Cul5$_{NTD}$ complex, measurements were taken at six wave heights (7.0, 7.5, 8.0, 8.5, 9.0, and 9.5 V). The reported collision cross section (CCS) values are an average of the data recorded over all of the wave heights. The CCS calibration procedure used was described previously[31] and involved validation through the use of CCS data from other known protein ions.[32] The drift times for all charge states were obtained using MassLynx and DriftScope (Waters).

Calculations of the Theoretical Collision Cross Sections (CCS) from Atomic-Level Structures. To compare the CCS values measured for ASB9−EloBC−Cul5$_{NTD}$ with their theoretical values, the atomic-level structure of the ASB9−EloBC−Cul5$_{NTD}$ quaternary complex was obtained by molecular modeling. The program used for the CCS calculation was DriftScope,[33] which is based on the projection approximation (PA) method.

Differential-Scanning Fluorimetry. Thermal-shift experiments were carried out in 96-well real-time PCR plates (LightCycler 480 Multiwell Plate 96, Roche) using a 100 μL total volume per sample, and each sample had a final concentration of 2.5× Sypro Orange (Sigma) in 50 mM HEPES, 100 mM NaCl, pH 7.5, and 1 mM TCEP. The plates were covered with the provided sealing foils, briefly vortexed, and centrifuged for 2 min. The temperature was increased from 37 to 95 °C at a rate of 1 °C/min using a LightCycler 480 real-time PCR system (Roche). The protein melting curves were plotted as the fluorescence intensity (RFU) versus temperature, and the melting temperatures were identified by the minimum of each curve's derivative ($-dRFU/dT$). To examine the thermal stability of ASB9−EloBC, the melting curve of 2 μM ASB9−EloBC was monitored in the presence of Cul5$_{NTD}$ at final concentrations of 8, 4, 2, 1, 0.5, and 0.25 μM (doubling dilutions).

Isothermal-Titration Calorimetry. Isothermal-titration calorimetry experiments were performed with a MicroCal ITC$_{200}$ microcalorimeter (GE Healthcare). Cul5$_{NTD}$ (450 μM) was titrated into ASB9−EloBC (60 μM) in the sample cell using 19 injections of 2 μL each (120 s spacing between injections with a 500 rpm stirring speed) at 288, 293, 298, and 303 K. Cul2$_{NTD}$ (450 μM) was titrated into ASB9−EloBC (60 μM) at 298 K. All protein solutions were equilibrated in 50 mM HEPES, 100 mM NaCl, pH 7.5, and 1 mM TCEP prior to performing the titration experiments. Control experiments were
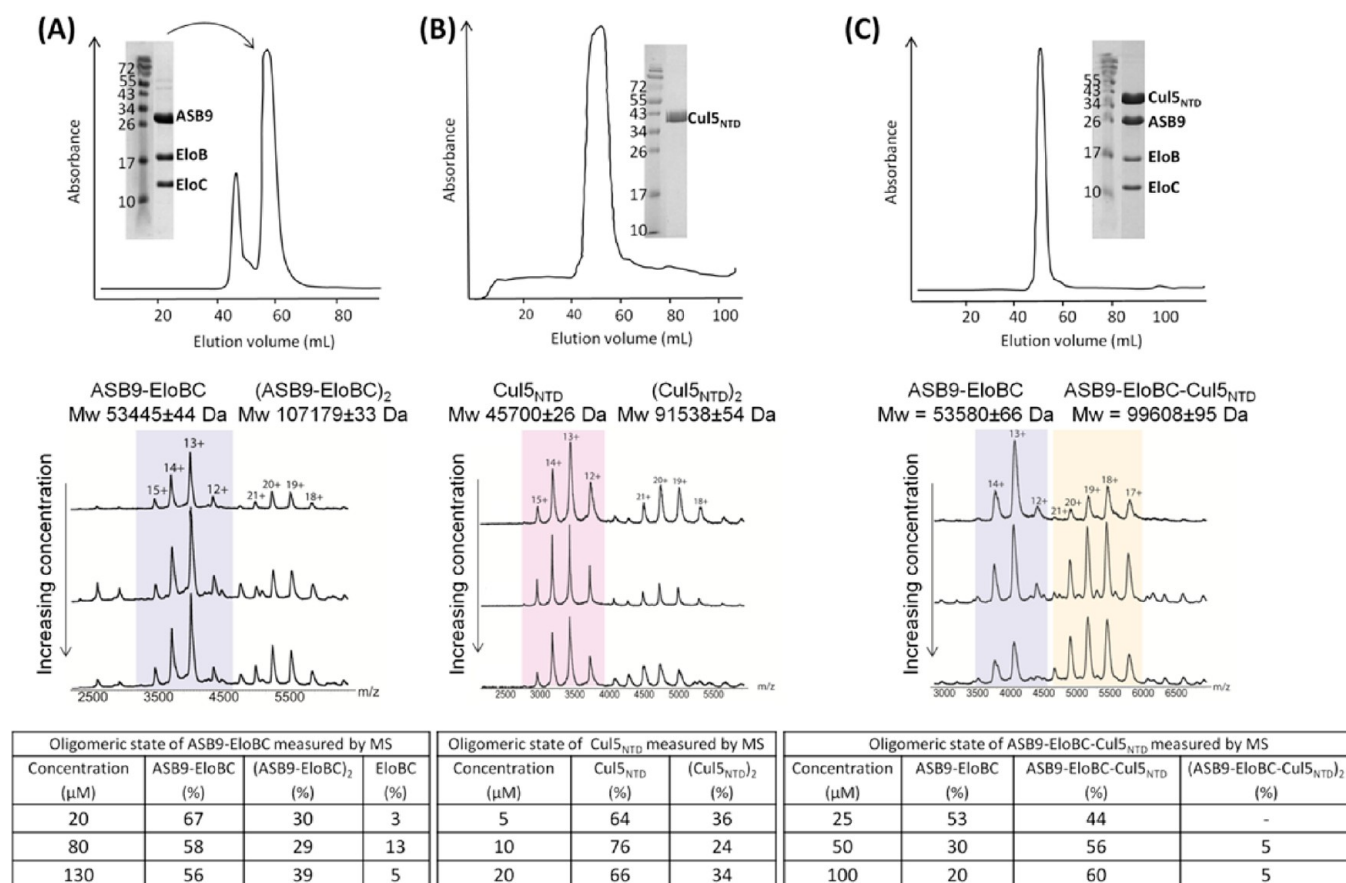
Figure 2. ASB9–EloBC binds Cul5$_{NTD}$ to form a monomeric quaternary complex, ASB9–EloBC–Cul5$_{NTD}$. Size-exclusion gel filtration traces, denaturing SDS-PAGE, and native mass spectra are shown for ASB9–EloBC (A), Cul5$_{NTD}$ (B), and ASB9–EloBC–Cul5$_{NTD}$ (C). The tables below the spectra quantify the amount of the different species in each protein sample, as observed by nanoESI–MS at three concentrations. The first peak in the gel-filtration trace for ASB9–EloBC (A) is due to a contaminant protein resulting from the expression in *E. coli* and was removed during this purification. Only one gel-filtration peak is observed upon mixing equimolar amounts of ASB9–EloBC and Cul5$_{NTD}$ (C), suggesting the formation of quaternary complex ASB9–EloBC–Cul5$_{NTD}$.

performed by titrating Cul5$_{NTD}$ (450 μM) into buffer. Data analyses for the ITC experiments were performed using the MicroCal Origin 7.0 software package. The dissociation constant, K_d, binding enthalpy, ΔH, and stoichiometry, n, values were calculated by fitting the calorimetric data curves to a standard one-set-of-sites model. The values quoted in Figure 3D are the mean of triplicate experiments, and the errors are the standard deviations of the mean.

Molecular Modeling of ASB9–EloBC–Cul5$_{NTD}$. A structural model of the ASB9–EloBC–Cul5$_{NTD}$ quaternary complex was obtained in Pymol using the crystal structure of Fbox^{Skp2}–Skp1–Cul1$_{NTD}$ (PDB 1LDK)[34] as a template. To construct the model, the ASB9–EloBC crystal structure (PDB 3ZKJ) was first superimposed as a rigid body on the template by aligning its EloC subunit with the Skp1 subunit of Fbox^{Skp2}–Skp1–Cul1$_{NTD}$. Second, the crystal structure of Cul5$_{NTD}$ (PDB 2WZK) was superimposed as a rigid body to the template by aligning its first α-helical bundle domain (residues 15–146) with the corresponding region of Cul1$_{NTD}$ (residues 20–170).

■ RESULTS

ASB9 Forms a Stable Complex with Elongin B–Elongin C. To monitor the formation of the ternary complex among ASB9 and Elongin B–Elongin C (EloBC), the three proteins were coexpressed in *Escherichia coli*, and the complex

purified using Ni-affinity chromatography and size-exclusion gel filtration followed by analysis using native nanoelectrospray ionization mass spectrometry (nanoESI–MS). Native nano-ESI–MS is one of the most accurate and sensitive techniques for determining the molecular weight and stoichiometry of large intact protein complexes.[35,36] ASB9–EloBC was examined by mass spectrometry at three concentrations (20, 80, and 130 μM), all of which supported the existence of the ternary protein complex (expected molecular weight calculated from protein sequences, 53 447 Da). The peaks for the ternary ASB9–EloBC complex appear in the range 3500–4000 m/z, with four (12$^+$ to 15$^+$) charge states (Figure 2A). The presence of a dimeric species (ASB9–EloBC)$_2$ with a molecular weight of 107 kDa was also observed at each concentration in the 4800–6000 m/z range with four charge states (18$^+$ to 21$^+$). The low population of dimeric species would imply only a weak interaction; however, the monomer–dimer distribution over the range of concentrations could not be fitted to a binding isotherm, suggesting the observed dimerization could be due to an artifact of the nanoESI–MS. Additionally, this dimerization was not observed by size-exclusion chromatography, although there was a contaminant protein with a molecular weight of ~75 kDa present arising from the expression in *E. coli* (Figure 2A). This contaminant was removed by gel filtration to provide purified ASB9–EloBC for biophysical analysis.
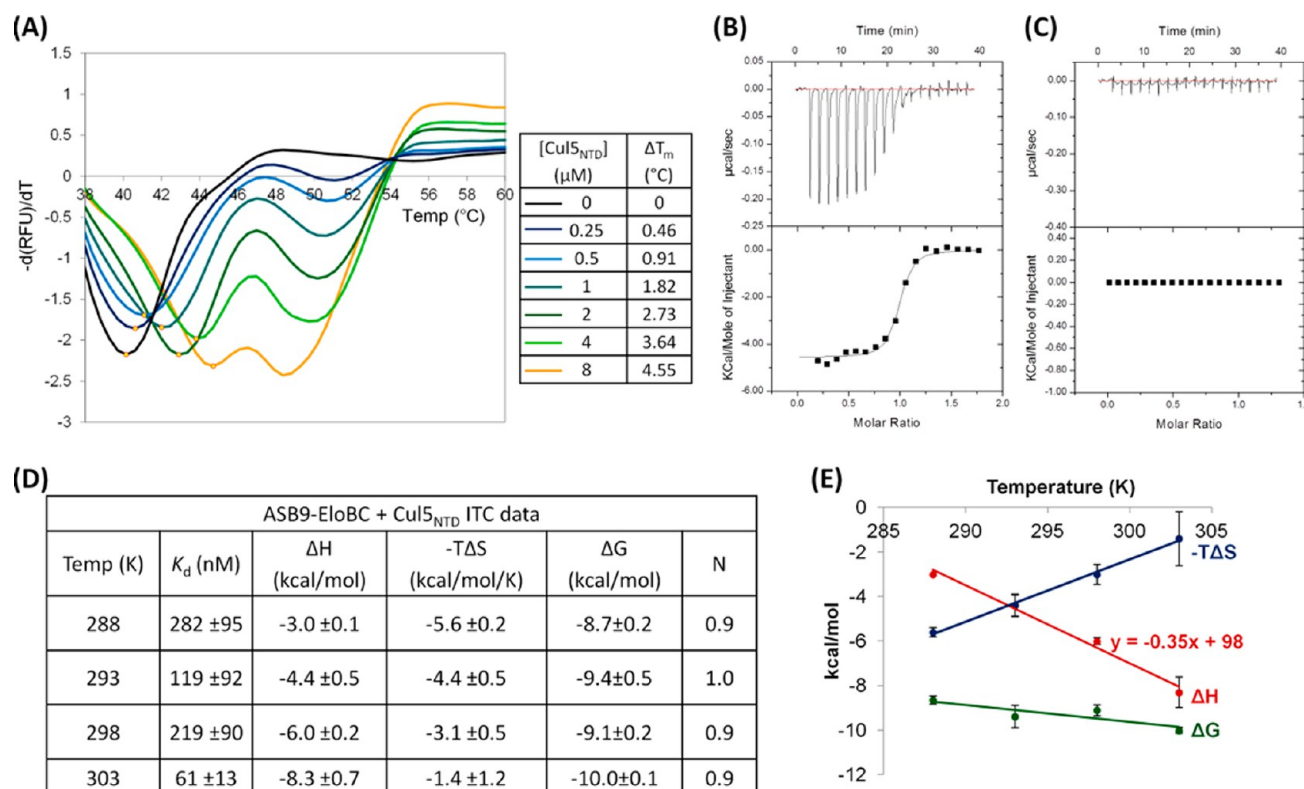
Figure 3. ASB9−EloBC binds with high affinity to Cul5$_{NTD}$ and specifically over Cul2$_{NTD}$, and binding increases the stability of ASB9−EloBC. (A) Differential-scanning fluorimetry curves for ASB9−EloBC (2 μM, T_m = 40.2 °C) in the presence of increasing concentrations of Cul5$_{NTD}$ (max ΔT_m = 4.6 °C). The minima observed between 48 and 52 °C are due to the melting of Cul5$_{NTD}$, and they increase in intensity with increasing Cul5$_{NTD}$ concentrations. (B) Example ITC titration of Cul5$_{NTD}$ (450 μM) into ASB9−EloBC (60 μM) at 293 K. (C) ITC titration of Cul2$_{NTD}$ (450 μM) into ASB9−EloBC (60 μM), confirming that ASB9−EloBC does not bind to Cul2. (D) Thermodynamic data for the ASB9−EloBC + Cul5$_{NTD}$ interaction obtained from ITC experiments performed at various temperatures. (E) Thermodynamic parameters ΔH, $-T\Delta S$, and ΔG are plotted against temperature (T). The slope of the linear fit of ΔH against T corresponds to the ΔC_p of ASB9−EloBC−Cul5$_{NTD}$ complex formation (−0.35 kcal mol^{-1} K^{-1}).

The Cullin 5 N-terminal domain (Cul5$_{NTD}$, residues 1−386) was also expressed in *E. coli*, purified by Ni-affinity chromatography and size-exclusion gel filtration, and examined by nanoESI−MS. Cul5$_{NTD}$ is able to fold independently in solution and is known to contain the binding site for the adaptor EloBC and the SOCS-box-containing substrate recognition subunits of CRLs; therefore, this construct was used for the in vitro analysis rather than full-length Cullin 5.[37,38] The construct contains two point mutations, V341R and L345D, to increase the solubility and stability of recombinant Cul5$_{NTD}$ (expected molecular weight from protein sequences, 45 690 Da). Cul5$_{NTD}$ eluted at a smaller elution volume during size-exclusion chromatography (54 mL) than ASB9−EloBC (57 mL) despite having a lower molecular weight (Figure 2), which is likely a result of its elongated shape (Figure 1B), causing it to behave as a larger protein by gel filtration. As shown in Figure 2B, monomeric Cul5$_{NTD}$ appears in the mass spectrum in the range 2800−4000 m/z with four charge states (12$^+$ to 15$^+$). Additionally, dimeric Cul5$_{NTD}$ was present at the three concentrations tested (5, 10, and 20 μM). As in the case of ASB9−EloBC, the monomer−dimer distribution could not be fitted to a binding isotherm and dimerization was not observed by size-exclusion chromatography, suggesting that Cul5$_{NTD}$ is predominantly monomeric at physiological pH.

ASB9−EloBC and the Cullin 5 N-Terminal Domain Bind to Form a Monomeric Multisubunit Protein Complex. To investigate further the assembly of the E3

CRL protein subunits, the ASB9−EloBC ternary complex and Cul5$_{NTD}$ were mixed in equimolar amounts at room temperature, and the solution was purified by size-exclusion chromatography. The resulting species eluted as a single peak at elution volume 50 mL (Figure 2C), which is consistent with the formation of a protein complex that is larger than ASB9−EloBC (elution volume 57 mL) or Cul5$_{NTD}$ (elution volume 54 mL). The formation of quaternary complex ASB9−EloBC−Cul5$_{NTD}$ was confirmed by native mass spectrometry analysis. The main species showed an observed mass of ∼99 500 Da (expected molecular weight from protein sequences, 99 137 Da), corresponding to ASB9−EloBC forming a 1:1 complex with Cul5$_{NTD}$ (Figure 2C), although unbound ASB9−EloBC was also present. The proportion of quaternary ASB9−EloBC−Cul5$_{NTD}$ relative to ASB9−EloBC increased with increasing protein concentrations, suggesting that ASB9−EloBC and ASB9−EloBC−Cul5$_{NTD}$ are in equilibrium with each other and that the equilibrium shifts toward ASB9−EloBC−Cul5$_{NTD}$ dissociation at lower protein concentrations. Only negligible amounts of ASB9−EloBC−Cul5$_{NTD}$ dimer were observed, and this disappeared at higher dilutions, implying that the ASB9−EloBC−Cul5$_{NTD}$ CRL assembles as a specific monomeric complex.

ASB9−EloBC Binds to Cul5$_{NTD}$ with High Affinity but Not to Cul2$_{NTD}$. To investigate the effect of Cul5$_{NTD}$ binding on ASB9−EloBC protein stability, we performed differential-scanning fluorimetry experiments. The melting point (T_m) of
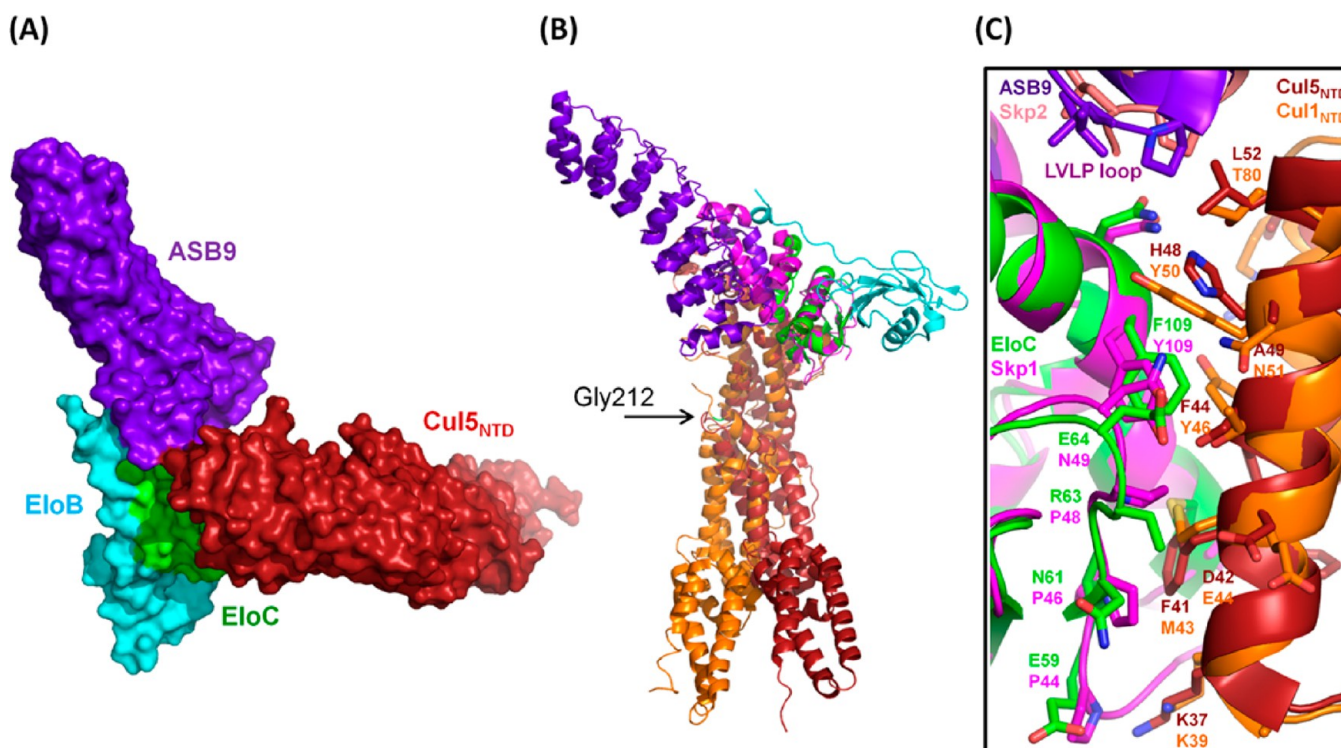
Figure 4. Structural model of the quaternary complex ASB9−EloBC−Cul5$_{NTD}$. The model was constructed using the crystal structure of Fbox^{Skp2}−Skp1−Cul1$_{NTD}$ as a template (PDB 1LDK).[34] The Cul5$_{NTD}$ crystal structure (PDB 2WZK) was aligned with Cul1$_{NTD}$, and EloC of the ASB9−EloBC crystal structure (PDB 3ZKJ) was aligned with Skp1 of the Fbox^{Skp2}−Skp1−Cul1$_{NTD}$ structure. ASB9 is shown in purple, EloC, in green, EloB, in cyan, Cul5$_{NTD}$, in red, Cul1$_{NTD}$, in orange, Skp1, in dark pink, and Fbox^{Skp2}, in light pink. (A) Surface representation of the ASB9−EloBC−Cul5$_{NTD}$ quaternary complex. (B) Structural alignment of ASB9−EloBC−Cul5$_{NTD}$ with Fbox^{Skp2}−Skp1−Cul1$_{NTD}$ showing the variation in the Cullin NTD orientations. The kink at Cul1$_{NTD}$ residue Gly212 is labeled. (C) Close-up structural alignment of ASB9−EloBC−Cul5$_{NTD}$ with Fbox^{Skp2}−Skp1−Cul1$_{NTD}$ showing the high structural conservation at the interface between the adaptor protein (Skp1/EloC) and Cullin (Cul1/Cul5, respectively).

ASB9−EloBC in the absence of Cul5$_{NTD}$ is relatively low at 40.2 °C (Figure 3A), which is consistent with that observed for other ankyrin-repeat-domain-containing proteins, including Notch, p16, and IκBα.[39−41] Interestingly, the melting curve derivative of ASB9−EloBC contains just one minimum, suggesting that the ternary protein complex unfolds in a single-step process. Titration of the more stable Cul5$_{NTD}$ (T_m = 50.2 °C) increases the T_m of ASB9−EloBC (ΔT_m = 4.6 °C with a 4-fold excess of Cul5$_{NTD}$), indicating the enhanced stability of ASB9−EloBC upon Cul5$_{NTD}$ binding, which is consistent with the formation of the quaternary complex ASB9−EloBC−Cul5$_{NTD}$ (Figure 3A).

To gain further insights into the affinity and thermodynamics of the ASB9−EloBC and Cul5$_{NTD}$ interaction, we performed temperature-dependence studies using isothermal-titration calorimetry (Figure 3B,D). ASB9−EloBC was found to bind to Cul5$_{NTD}$ with a K_d value of 220 ± 90 nM at 298 K. This affinity is weaker than that previously reported for Cul5$_{NTD}$ binding to the ternary complexes between EloBC and SOCS-box fragments from SOCS2, SOCS4, SOCS5, SOCS6, and SOCS7 (K_d = 10−40 nM).[38] In part, this may be due to variations in the buffers and assay conditions used. However, it may also reflect the sequence deviation in the ASB9 Cul5-box (LVLP) from the canonical motif, LPXP (Figures 1C and S2), which is essential for the recruitment of Cul5.[21,42,43] The stoichiometry of binding is 1:1 ASB9−EloBC/Cul5$_{NTD}$, which is consistent with the native mass spectrometry analysis. The binding of ASB9−EloBC to Cul5$_{NTD}$ is favorable both

enthalpically (ΔH = −6.0 ± 0.2 kcal mol^{-1}) and entropically ($-T\Delta S$ = −3.1 ± 0.5 kcal mol^{-1}) at 298 K. At increased temperatures, ΔH dominates binding as $-T\Delta S$ becomes less favorable (at 303 K, ΔH = −8.3 ± 0.7 kcal mol^{-1} and $-T\Delta S$ = −1.4 ± 1.2 kcal mol^{-1}), and conversely, at 288 K entropy drives complex formation (ΔH = −3.0 ± 0.1 kcal mol^{-1} and $-T\Delta S$ = −5.6 ± 0.2 kcal mol^{-1}). However, ΔG does not show significant variation with temperature as a result of enthalpy−entropy compensation (Figure 3D,E).

We plotted ΔH against temperature to calculate the change in heat capacity (ΔC_p) upon ASB9−EloBC−Cul5$_{NTD}$ complex formation, resulting in ΔC_p = −0.35 kcal mol^{-1} K^{-1} (Figure 3E). This value is very similar to that previously reported for the Cul5$_{NTD}$ interaction with the ternary complex formed among the SOCS-box-containing C-terminal domain of HIV-1 Vif and EloBC (Vif$_{CTD}$−EloBC), which was determined to be −0.30 kcal mol^{-1} K^{-1} using an analogous method of temperature-dependent ITC titrations.[44] This consistency between ΔC_p values suggests that Cul5$_{NTD}$ binding to various SOCS-box−EloBC complexes occurs via similar interactions, which may be conserved in other ECS-type CRLs.

To address the specificity of the ASB9−EloBC and Cul5 interaction, we performed isothermal-titration calorimetry studies of ASB9−EloBC with the Cullin 2 N-terminal domain (Cul2$_{NTD}$, residues 8−384). Cul2 also forms Cullin-RING E3 ubiquitin ligase complexes using EloBC as the adaptor proteins, but is believed to interact with proteins containing VHL-box domains rather than SOCS-box motifs.[42,43] As expected, no
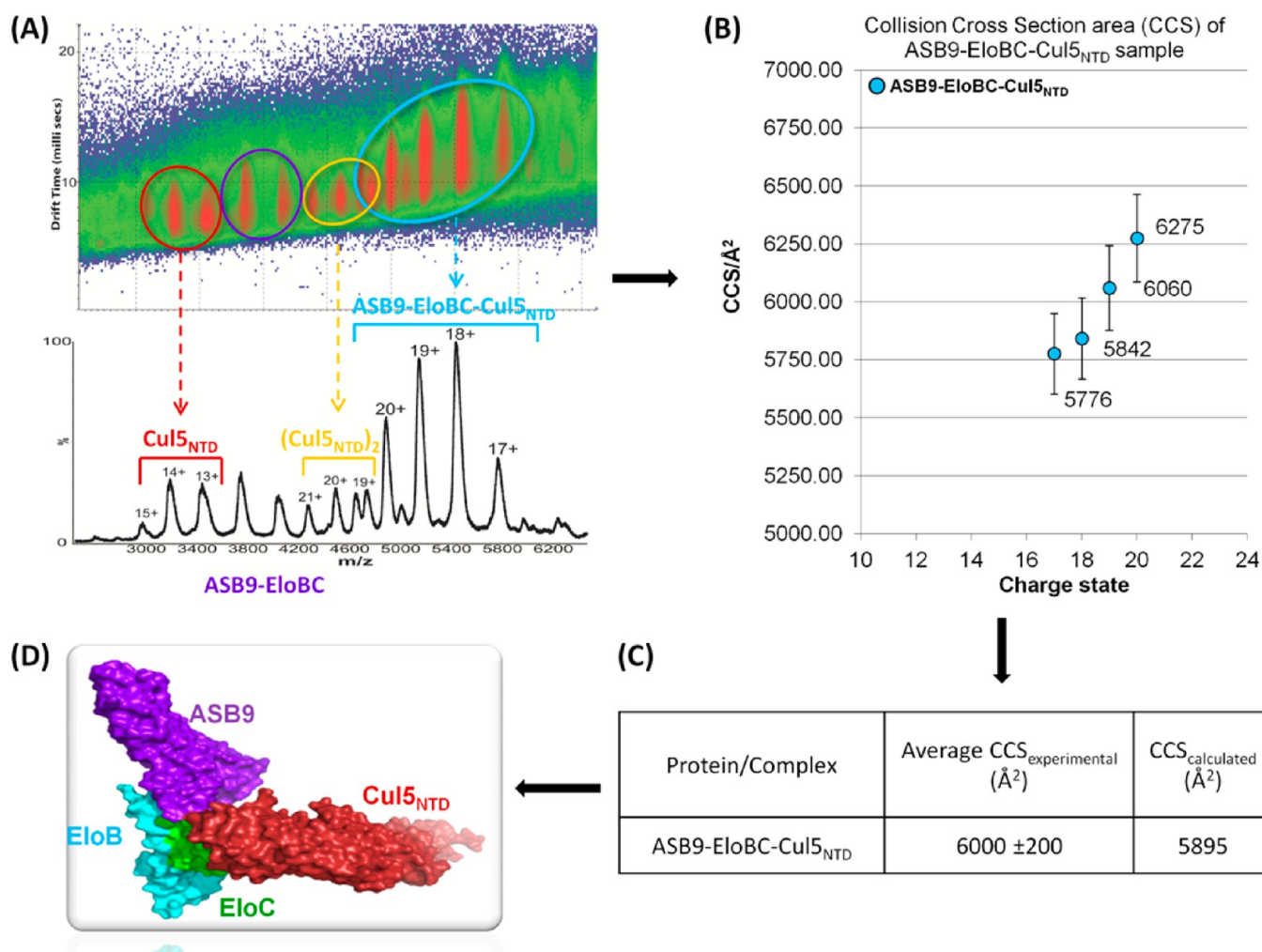
Figure 5. Ion-mobility mass spectrometry data for the ASB9−EloBC−Cul5$_{NTD}$ quaternary complex. (A) Native mass spectrum and ion-mobility drift-time plot of the ASB9−EloBC−Cul5$_{NTD}$ sample. The quaternary complex (cyan) partially dissociates. ASB9−EloBC (purple) and Cul5$_{NTD}$ (monomeric (red) and dimeric (yellow)) are also present but are separated by their varying drift times. (B) Experimentally measured collision cross section (CCS) areas of four charge states (17$^+$ to 20$^+$) of ASB9−EloBC−Cul5$_{NTD}$. (C) Average CCS values for the ASB9−EloBC−Cul5$_{NTD}$ quaternary complex were determined to be 6000 ± 200 Å^2, which is in good agreement with that calculated (5895 Å^2) from the model shown in panel D.

binding was observed for the titration of Cul2$_{NTD}$ into ASB9−EloBC by ITC (Figure 3C). This suggests that CRL formation of ASB9−EloBC is specific for Cul5 over Cul2.

Molecular Modeling Provides the First Insights into the Structure of the N-Terminal Region of an ASB-Containing Cul5 E3 Ubiquitin Ligase. We constructed a structural model of the ASB9−EloBC−Cul5$_{NTD}$ quaternary complex using the published crystal structure of the homologous Fbox^{Skp2}−Skp1−Cul1$_{NTD}$ complex as a template.[34] The first α-helical bundle of the crystal structure of Cul5$_{NTD}$ (PDB 2WZK) was aligned with the corresponding region of Cul1$_{NTD}$ (sequence identity 29%, rmsd of all atoms 2.31 Å), whereas the EloC subunit of the ASB9−EloBC ternary-complex crystal structure (PDB 3ZKJ) was aligned with the homologous Skp1 subunit (sequence identity 38%, rmsd of all atoms 1.19 Å) to give the quaternary complex shown in Figure 4A. Similar models of other ECS-type CRL quaternary complexes have previously been reported, including those for SOCS2−EloBC−Cul5,[45] RAR3−EloBC−Cul5,[42] HIV-1 Vif−EloBC−Cul5,[46] and VHL−EloBC−Cul2.[42] Our model shows

that the Cul5$_{NTD}$ stalk is oriented in the opposite direction relative to the ankyrin repeats of ASB9.

The superposition of our model onto the Fbox^{Skp2}−Skp1−Cul1$_{NTD}$ complex shows that although Cul1$_{NTD}$ and Cul5$_{NTD}$ have the same overall structure there is variation in the relative orientation of their α-helix bundles (Figure 4B). This likely reflects the inherent flexibility of the Cullins that has been predicted computationally by Liu et al.[47] and is proposed to be relevant to the allosteric regulations of CRLs. In fact, the Cul1$_{NTD}$ kink observed in the structural alignment with Cul5$_{NTD}$ occurs near Gly 212 on repeat 2, which is a residue that was previously observed to act as a hinge during molecular dynamics simulations of Cul1$_{NTD}$.[47] However, there is high structural conservation at the interface between Cullin and the adaptor-box proteins (Figure 4C).

We used this model together with the individual crystal structures of ASB9−EloBC and Cul5$_{NTD}$ to calculate the change in solvent-accessible surface area (ΔSASA) upon ASB9−EloBC−Cul5$_{NTD}$ complex formation. Using PyMOL, ΔSASA of ASB9−EloBC and Cul5$_{NTD}$ binding was calculated to be −1238 Å^2, of which 437 Å^2 is due to the burial of polar

atoms and 801 Å^2 from the burial of hydrophobic regions (Figure S3). This ΔSASA value is of a similar magnitude to those determined for the interface between Fbox^{Skp2}–Skp1 and Cul1$_{NTD}$ (1780 Å^2, PDB 1LDK),[34] the BTB^{SPOP}–Cul3$_{NTD}$ binding interface (825 Å^2, PDB 4EOZ),[18] and the KLHL11–Cul3$_{NTD}$ interface (1508 Å^2, PDB 4AP2),[19] supporting the relevance of our model and further indicating that many CRL complexes assemble via a common topology at the Cul$_{NTD}$–adaptor interface.

Ion-Mobility Data Support Our Modeled Structure of the ASB9–EloBC–Cul5$_{NTD}$ Quaternary Complex. Attempts to obtain the atomic-level structure of the ASB9–EloBC–Cul5$_{NTD}$ quaternary complex in our laboratory have so far been unsuccessful, and previously reported models of quaternary ECS-type CRL complexes have not been experimentally validated. To provide structural validation of our quaternary complex model, ion-mobility mass spectrometry (IM–MS) experiments were performed on the ASB9–EloBC–Cul5$_{NTD}$ complex purified by size-exclusion chromatography. Under native conditions, drift times were measured for four charge states (17$^+$ to 20$^+$) of the intact monomeric heterocomplex ASB9–EloBC–Cul5$_{NTD}$ (Figure 5), and the average collision cross section (CCS) was determined to be 6000 ± 200 Å^2 (Figure 5B,C), which is in very good agreement with the CCS calculated from the model of ASB9–EloBC–Cul5$_{NTD}$ (5895 Å^2). This implies that our model reflects a highly probable conformation of the quaternary complex and therefore provides insight into the physiological structure of this multimeric system.

■ DISCUSSION

ASB9 is the substrate-recognition subunit of a Cullin-RING E3 ubiquitin ligase complex and is part of the 18-member ASB protein family. To date, little is known about the interactions and biological functions of this family, and there have previously been no reported in vitro biophysical studies on the structural assembly of any of these proteins as part of a CRL complex. Here, we provide the first evidence that ASB9–EloBC binds to Cul5$_{NTD}$ with high affinity to form a monomeric multisubunit protein complex with an analogous structure to that of other CRLs.

The majority of Cullin-RING ligases are believed to function as monomeric species, although it is known that some can act as dimers, for example, SPOP–Cullin3,[18,48] KLHL11–Cullin3,[19] SCF^{Fbx4},[20] and SCF^{Cdc4}.[17] Our data suggest that the ASB9–EloBC–Cul5 CRL functions as a canonical monomeric heterocomplex because the quaternary species ASB9–EloBC–Cul5$_{NTD}$ was only observed in a monomeric state by size-exclusion chromatography and native mass spectrometry. Cul5$_{NTD}$ and ASB9–EloBC were able to form dimeric species in native mass spectrometry analysis; however, this is likely to be due to a nonspecific nanoESI–MS artifact; Cul1, Cul3, and Cul4a have all been reported to form homodimers in cells, but this was not previously observed for Cul2 and Cul5.[15]

ASB9 is stable when complexed to EloBC, but we were unable to express it recombinantly alone. This instability of the free protein has also been reported for ASB2.[22] The ankyrin-repeat domain of ASB9 (ASB9 isoform 2, ASB9-2) has recently been crystallized and the structure solved,[49] implying that this species is stable in solution. Therefore, it is likely that it is the SOCS-box domain or the linker region of ASB9 and other ASB proteins that causes the instability of the noncomplexed species. The fact that unbound ASB9 does not seem to be favorable in

solution suggests that it is likely to first form a long-lived complex with EloBC before recruiting Cullin 5 to form the active CRL system in cells. This is also indicated by native mass spectrometry analyses of the quaternary ASB9–EloBC–Cul5$_{NTD}$ complex; ASB9–EloBC–Cul5$_{NTD}$ readily dissociates into ASB9–EloBC and Cul5$_{NTD}$, but only small amounts of further subunit dissociation within ASB9–EloBC were seen.

ASB9–EloBC binds to Cul5$_{NTD}$ with a K_d value of ∼200 nM at 298 K. This is approximately 5–20-fold weaker than the affinities previously reported for other SOCS-box–EloBC complexes binding to Cul5$_{NTD}$.[38] The SOCS-box domain contains a Cullin 5-binding motif $\varphi XXLP\varphi PXX\varphi XX[YF][LI]$ (φ is a hydrophobic residue and X is any residue),[43] and the SOCS proteins that exhibit K_d <100 nM for Cul5$_{NTD}$ all contain the canonical sequence LPLP at the key positions 4–7 of this motif (Figure S2). However, in ASB9 this is replaced with LVLP, possibly leading to the apparent weaker affinity for Cul5. SOCS1 (IPLN) and SOCS3 (LPGP) also show deviations from this motif (Figure S2), and they bind Cul5$_{NTD}$ with K_d values of 1 μM and 105 nM, respectively,[38] which further indicates that mutations in these positions can cause a reduction in the affinity for Cul5. In addition to ASB9, ASB4, ASB5, ASB11, ASB12, and ASB13 show deviations from the canonical Cul5-box sequence, although the majority of the ASB family contains LPLP in positions 4–7 (Figure S4). A weaker affinity for Cul5$_{NTD}$ and therefore reduced CRL complex formation may have consequences for the efficiency of ASB9-dependent ubiquitination in cells because ASB9 will be less effective at competing for Cullin 5 than other EloBC–Cul5 binding proteins. This may play a role in the regulation of ASB9-mediated polyubiquitination of its substrates. Interestingly, both SOCS1 and SOCS3 are believed to act as suppressors of cytokine signaling by an additional SOCS-box-independent mechanism, explaining why Cul5$_{NTD}$ affinity need not be so high for these proteins.[38] The SOCS proteins that act only through SOCS-box-dependent ubiquitination and substrate degradation all have K_d <50 nM. This raises the possibility that ASB9 could have an additional role to that of CRL substrate-binding protein in vivo, although this awaits further study.

The ΔC_p value of ASB9–EloBC–Cul5$_{NTD}$ complex formation was measured to be −0.35 kcal mol^{-1} K^{-1} by ITC. The negative value of ΔC_p indicates that the surface buried on complex formation is dominated by hydrophobic interactions.[50] The ΔC_p value may be used to calculate an approximation of the change in solvent-accessible surface area (ΔSASA) of a protein interaction using the equation[51]

$$\Delta SASA\ (\text{Å}^2) = \frac{\Delta C_p\ (\text{cal mol}^{-1}\ \text{K}^{-1})}{-0.146}$$

This results in a ΔSASA value of 2397 Å^2, which is about twice the value calculated from the structural model of ASB9–EloBC–Cul5$_{NTD}$. This variation in ΔSASA is likely partly due to the crude method used in converting ΔC_p to ΔSASA but may also indicate a conformational change in ASB9–EloBC and/or Cul5$_{NTD}$ that is not accounted for by the static crystal-structure-based model. However, because the quaternary complex model shows good agreement with ion-mobility experimental measurements, any conformational variation is likely to be small and localized at the quaternary complex interface.

It is interesting to note that in the structural model of the ASB9–EloBC–Cul5$_{NTD}$ complex the ankyrin groove of the

ASB9 ankyrin-repeat domain faces the C-terminal region of $Cul5_{NTD}$ where the RING-box protein and ubiquitin-loaded E2 enzyme would be located in the full CRL complex. The ankyrin groove of ankyrin-repeat domains is a common binding site for protein−protein interactions,[52,53] suggesting that this region of ASB9 may bind the substrate and orient it in a suitable way to allow polyubiquitination.

We have reported the first biophysical characterization of the components of an ASB CRL complex as well as the first experimentally validated structural information for the assembly of the quaternary N-terminal region of an ASB CRL. We provide a platform for further investigation of the assembly mechanisms of ASB proteins and other ECS-type CRLs, which will assist in the development of chemical probes to examine the biological functions and therapeutic potential of this important protein family. Recent progress in identifying small molecules targeting binding surfaces and interfaces of CRLs, such as SCF^{Cdc4},[54] ECS^{VHL},[55] and SCF^{Skp2},[56] suggests that other E3 ligases, including the ASB CRL family, may be also amenable to modulation by drug-like small molecules.

■ ASSOCIATED CONTENT

Ⓢ Supporting Information

SDS-PAGE analysis of $Cul2_{NTD}$; sequence alignment of the SOCS-box regions of SOCS proteins 1−7, ASB9, and HIV Vif; ITC data for the titration of $Cul5_{NTD}$ into various SOCS-box/ EloBC proteins; solvent-accessible surface area (SASA) calculated from crystal structures; and sequence alignment of the SOCS-box domains of all 18 members of the ASB protein family. This material is available free of charge via the Internet at http://pubs.acs.org.

■ AUTHOR INFORMATION

Corresponding Author

*Phone: +44 1382 386230. Fax: +44 1382 386373. E-mail: a. ciulli@dundee.ac.uk.

Present Address

†College of Life Sciences, Division of Biological Chemistry and Drug Discovery, University of Dundee, James Black Centre, Dow Street, Dundee, DD1 5EH, United Kingdom. Dr. Inge Van Molle: VIB, Department of Structural Biology, Structural Biology Brussels, Vrije Universiteit Brussel, Building E, room 4.16, Pleinlaan 2, 1050 Brussels, Belgium.

Author Contributions

A.C. designed the research. J.T. and D.M.V. performed the experiments. All authors analyzed data. J.T. and A.C. wrote the manuscript with suggestions from all authors.

Notes

The authors declare no competing financial interest.

■ ACKNOWLEDGMENTS

■ ABBREVIATIONS

SOCS, suppressors of cytokine signaling; ASB9, ankyrin-repeat and SOCS-box protein 9; EloB, elongin B; EloC, elongin C; EloBC, elongin B elongin C complex; Cul, Cullin; RING, really interesting new gene; Rbx, RING-box protein; CRL, Cullin RING ligase; ECS, EloBC−Cullin−SOCS-box; SRS, substrate recognition subunit; NTD, N-terminal domain; VHL, Von Hippel-Lindau; BTB, Bric-a-brac, Tramtrack and Broad complex; Skp, S-phase, kinase-associated protein; RMSD, root-mean-square deviation; IM−MS, ion-mobility mass spectrometry; CCS, collision cross section

■ REFERENCES

(1) Hershko, A., and Ciechanover, A. (1998) The ubiquitin system. *Annu. Rev. Biochem. 67*, 425−479.

(2) Pickart, C. M. (2001) Mechanisms underlying ubiquitination. *Annu. Rev. Biochem. 70*, 503−533.

(3) Glickman, M. H., and Ciechanover, A. (2002) The ubiquitin-proteasome proteolytic pathway: destruction for the sake of construction. *Physiol. Rev. 82*, 373−428.

(4) Deshaies, R. J., and Joazeiro, C. A. (2009) RING domain E3 ubiquitin ligases. *Annu. Rev. Biochem. 78*, 399−434.

(5) Jackson, S., and Xiong, Y. (2009) CRL4s: the CUL4-RING E3 ubiquitin ligases. *Trends Biochem. Sci. 34*, 562−570.

(6) Soucy, T. A., Smith, P. G., Milhollen, M. A., Berger, A. J., Gavin, J. M., Adhikari, S., Brownell, J. E., Burke, K. E., Cardin, D. P., Critchley, S., Cullis, C. A., Doucette, A., Garnsey, J. J., Gaulin, J. L., Gershman, R. E., Lublinsky, A. R., McDonald, A., Mizutani, H., Narayanan, U., Olhava, E. J., Peluso, S., Rezaei, M., Sintchak, M. D., Talreja, T., Thomas, M. P., Traore, T., Vyskocil, S., Weatherhead, G. S., Yu, J., Zhang, J., Dick, L. R., Claiborne, C. F., Rolfe, M., Bolen, J. B., and Langston, S. P. (2009) An inhibitor of NEDD8-activating enzyme as a new approach to treat cancer. *Nature 458*, 732−736.

(7) Petroski, M. D., and Deshaies, R. J. (2005) Function and regulation of cullin-RING ubiquitin ligases. *Nat. Rev. Mol. Cell Biol. 6*, 9−20.

(8) Zimmerman, E. S., Schulman, B. A., and Zheng, N. (2010) Structural assembly of cullin-RING ubiquitin ligase complexes. *Curr. Opin. Struct. Biol. 20*, 714−721.

(9) Sarikas, A., Hartmann, T., and Pan, Z. Q. (2011) The cullin protein family. *Genome Biol. 12*, 220.

(10) Skowyra, D., Craig, K. L., Tyers, M., Elledge, S. J., and Harper, J. W. (1997) F-box proteins are receptors that recruit phosphorylated substrates to the SCF ubiquitin-ligase complex. *Cell 91*, 209−219.

(11) Xu, L., Wei, Y., Reboul, J., Vaglio, P., Shin, T. H., Vidal, M., Elledge, S. J., and Harper, J. W. (2003) BTB proteins are substrate-specific adaptors in an SCF-like modular ubiquitin ligase containing CUL-3. *Nature 425*, 316−321.

(12) Lonergan, K. M., Iliopoulos, O., Ohh, M., Kamura, T., Conaway, R. C., Conaway, J. W., and Kaelin, W. G., Jr. (1998) Regulation of hypoxia-inducible mRNAs by the von Hippel-Lindau tumor suppressor protein requires binding to complexes containing elongins B/C and Cul2. *Mol. Cell. Biol. 18*, 732−741.

(13) Kamura, T., Sato, S., Haque, D., Liu, L., Kaelin, W. G., Jr., Conaway, R. C., and Conaway, J. W. (1998) The Elongin BC complex interacts with the conserved SOCS-box motif present in members of the SOCS, ras, WD-40 repeat, and ankyrin repeat families. *Genes Dev. 12*, 3872−3881.

(14) Duda, D. M., Scott, D. C., Calabrese, M. F., Zimmerman, E. S., Zheng, N., and Schulman, B. A. (2011) Structural regulation of cullin-RING ubiquitin ligase complexes. *Curr. Opin. Struct. Biol. 21*, 257−264.

(15) Chew, E. H., Poobalasingam, T., Hawkey, C. J., and Hagen, T. (2007) Characterization of cullin-based E3 ubiquitin ligases in intact mammalian cells−evidence for cullin dimerization. *Cell. Signalling 19*, 1071−1080.

(16) Bosu, D. R., and Kipreos, E. T. (2008) Cullin-RING ubiquitin ligases: global regulation and activation cycles. *Cell Div. 3*, 7.

(17) Tang, X., Orlicky, S., Lin, Z., Willems, A., Neculai, D., Ceccarelli, D., Mercurio, F., Shilton, B. H., Sicheri, F., and Tyers, M. (2007) Suprafacial orientation of the SCFCdc4 dimer accommodates multiple geometries for substrate ubiquitination. *Cell 129*, 1165−1176.

(18) Errington, W. J., Khan, M. Q., Bueler, S. A., Rubinstein, J. L., Chakrabartty, A., and Prive, G. G. (2012) Adaptor protein self-assembly drives the control of a cullin-RING ubiquitin ligase. *Structure 20*, 1141−1153.

(19) Canning, P., Cooper, C. D., Krojer, T., Murray, J. W., Pike, A. C., Chaikuad, A., Keates, T., Thangaratnarajah, C., Hojzan, V., Marsden, B. D., Gileadi, O., Knapp, S., von Delft, F., and Bullock, A. N. (2013) Structural basis for Cul3 assembly with the BTB-Kelch family of E3 ubiquitin ligases. *J. Biol. Chem. 288*, 7803−7814.

(20) Li, Y., and Hao, B. (2010) Structural basis of dimerization-dependent ubiquitination by the SCF(Fbx4) ubiquitin ligase. *J. Biol. Chem. 285*, 13896−13906.

(21) Kohroki, J., Nishiyama, T., Nakamura, T., and Masuho, Y. (2005) ASB proteins interact with Cullin5 and Rbx2 to form E3 ubiquitin ligase complexes. *FEBS Lett. 579*, 6796−6802.

(22) Heuze, M. L., Guibal, F. C., Banks, C. A., Conaway, J. W., Conaway, R. C., Cayre, Y. E., Benecke, A., and Lutz, P. G. (2005) ASB2 is an Elongin BC-interacting protein that can assemble with Cullin 5 and Rbx1 to reconstitute an E3 ubiquitin ligase complex. *J. Biol. Chem. 280*, 5468−5474.

(23) Chung, A. S., Guan, Y. J., Yuan, Z. L., Albina, J. E., and Chin, Y. E. (2005) Ankyrin repeat and SOCS box 3 (ASB3) mediates ubiquitination and degradation of tumor necrosis factor receptor II. *Mol. Cell. Biol. 25*, 4716−4726.

(24) Li, J. Y., Chai, B., Zhang, W., Wu, X., Zhang, C., Fritze, D., Xia, Z., Patterson, C., and Mulholland, M. W. (2011) Ankyrin repeat and SOCS box containing protein 4 (Asb-4) colocalizes with insulin receptor substrate 4 (IRS4) in the hypothalamic neurons and mediates IRS4 degradation. *BMC Neurosci. 12*, 95.

(25) Debrincat, M. A., Zhang, J. G., Willson, T. A., Silke, J., Connolly, L. M., Simpson, R. J., Alexander, W. S., Nicola, N. A., Kile, B. T., and Hilton, D. J. (2007) Ankyrin repeat and suppressors of cytokine signaling box protein asb-9 targets creatine kinase B for degradation. *J. Biol. Chem. 282*, 4728−4737.

(26) Kwon, S., Kim, D., Rhee, J. W., Park, J. A., Kim, D. W., Kim, D. S., Lee, Y., and Kwon, H. J. (2010) ASB9 interacts with ubiquitous mitochondrial creatine kinase and inhibits mitochondrial function. *BMC Biol. 8*, 23-1−23-22.

(27) Zhong, L., Ge, K., Zu, J. C., Zhao, L. H., Shen, W. K., Wang, J. F., Zhang, X. G., Gao, X., Hu, W., Yen, Y., and Kernstine, K. H. (2008) Autoantibodies as potential biomarkers for breast cancer. *Breast Cancer Res. 10*, R40-1−R40-8.

(28) Tokuoka, M., Miyoshi, N., Hitora, T., Mimori, K., Tanaka, F., Shibata, K., Ishii, H., Sekimoto, M., Doki, Y., and Mori, M. (2010) Clinical significance of ASB9 in human colorectal cancer. *Int. J. Oncol. 37*, 1105−1111.

(29) Ruotolo, B. T., Giles, K., Campuzano, I., Sandercock, A. M., Bateman, R. H., and Robinson, C. V. (2005) Evidence for macromolecular protein rings in the absence of bulk water. *Science 310*, 1658−1661.

(30) Ruotolo, B. T., Hyung, S. J., Robinson, P. M., Giles, K., Bateman, R. H., and Robinson, C. V. (2007) Ion mobility-mass spectrometry reveals long-lived, unfolded intermediates in the dissociation of protein complexes. *Angew. Chem., Int. Ed. 46*, 8001−8004.

(31) Wood, T. D., Chorush, R. A., Wampler, F. M., 3rd, Little, D. P., O'Connor, P. B., and McLafferty, F. W. (1995) Gas-phase folding and unfolding of cytochrome c cations. *Proc. Natl. Acad. Sci. U.S.A. 92*, 2451−2454.

(32) Light-Wahl, K. J., Schwartz, B. L., and Smith, R. D. (1994) Observation of the noncovalent quaternary associations of proteins by electrospray ionization mass spectrometry. *J. Am. Chem. Soc. 116*, 5271−5278.

(33) Williams, J. P., Lough, J. A., Campuzano, I., Richardson, K., and Sadler, P. J. (2009) Use of ion mobility mass spectrometry and a collision cross-section algorithm to study an organometallic ruthenium anticancer complex and its adducts with a DNA oligonucleotide. *Rapid Commun. Mass Spectrom. 23*, 3563−3569.

(34) Zheng, N., Schulman, B. A., Song, L., Miller, J. J., Jeffrey, P. D., Wang, P., Chu, C., Koepp, D. M., Elledge, S. J., Pagano, M., Conaway, R. C., Conaway, J. W., Harper, J. W., and Pavletich, N. P. (2002) Structure of the Cul1-Rbx1-Skp1-F boxSkp2 SCF ubiquitin ligase complex. *Nature 416*, 703−709.

(35) Hernandez, H., and Robinson, C. V. (2007) Determining the stoichiometry and interactions of macromolecular assemblies from mass spectrometry. *Nat. Protoc. 2*, 715−726.

(36) Heck, A. J. (2008) Native mass spectrometry: a bridge between interactomics and structural biology. *Nat. Methods 5*, 927−933.

(37) Babon, J. J., Sabo, J. K., Soetopo, A., Yao, S., Bailey, M. F., Zhang, J. G., Nicola, N. A., and Norton, R. S. (2008) The SOCS box domain of SOCS3: structure and interaction with the elonginBC-cullin5 ubiquitin ligase. *J. Mol. Biol. 381*, 928−940.

(38) Babon, J. J., Sabo, J. K., Zhang, J. G., Nicola, N. A., and Norton, R. S. (2009) The SOCS box encodes a hierarchy of affinities for Cullin5: implications for ubiquitin ligase formation and cytokine signalling suppression. *J. Mol. Biol. 387*, 162−174.

(39) Croy, C. H., Bergqvist, S., Huxford, T., Ghosh, G., and Komives, E. A. (2004) Biophysical characterization of the free IkappaBalpha ankyrin repeat domain in solution. *Protein Sci. 13*, 1767−1777.

(40) Zweifel, M. E., and Barrick, D. (2001) Studies of the ankyrin repeats of the Drosophila melanogaster Notch receptor. 2. Solution stability and cooperativity of unfolding. *Biochemistry 40*, 14357−14367.

(41) Boice, J. A., and Fairman, R. (1996) Structural characterization of the tumor suppressor p16, an ankyrin-like repeat protein. *Protein Sci. 5*, 1776−1784.

(42) Kamura, T., Maenaka, K., Kotoshiba, S., Matsumoto, M., Kohda, D., Conaway, R. C., Conaway, J. W., and Nakayama, K. I. (2004) VHL-box and SOCS-box domains determine binding specificity for Cul2-Rbx1 and Cul5-Rbx2 modules of ubiquitin ligases. *Genes Dev. 18*, 3055−3065.

(43) Mahrour, N., Redwine, W. B., Florens, L., Swanson, S. K., Martin-Brown, S., Bradford, W. D., Staehling-Hampton, K., Washburn, M. P., Conaway, R. C., and Conaway, J. W. (2008) Characterization of Cullin-box sequences that direct recruitment of Cul2-Rbx1 and Cul5-Rbx2 modules to Elongin BC-based ubiquitin ligases. *J. Biol. Chem. 283*, 8005−8013.

(44) Salter, J. D., Lippa, G. M., Belashov, I. A., and Wedekind, J. E. (2012) Core-binding factor β increases the affinity between human Cullin 5 and HIV-1 Vif within an E3 ligase complex. *Biochemistry 51*, 8702−8704.

(45) Bullock, A. N., Debreczeni, J. E., Edwards, A. M., Sundstrom, M., and Knapp, S. (2006) Crystal structure of the SOCS2-elongin C-elongin B complex defines a prototypical SOCS box ubiquitin ligase. *Proc. Natl. Acad. Sci. U.S.A. 103*, 7637−7642.

(46) Stanley, B. J., Ehrlich, E. S., Short, L., Yu, Y., Xiao, Z., Yu, X. F., and Xiong, Y. (2008) Structural insight into the human immunodeficiency virus Vif SOCS box and its role in human E3 ubiquitin ligase assembly. *J. Virol. 82*, 8656−8663.

(47) Liu, J., and Nussinov, R. (2011) Flexible cullins in cullin-RING E3 ligases allosterically regulate ubiquitination. *J. Biol. Chem. 286*, 40934−40942.

(48) Zhuang, M., Calabrese, M. F., Liu, J., Waddell, M. B., Nourse, A., Hammel, M., Miller, D. J., Walden, H., Duda, D. M., Seyedin, S. N., Hoggard, T., Harper, J. W., White, K. P., and Schulman, B. A. (2009) Structures of SPOP-substrate complexes: insights into molecular architectures of BTB-Cul3 ubiquitin ligases. *Mol. Cell 36*, 39−50.

(49) Fei, X., Gu, X., Fan, S., Yang, Z., Li, F., Zhang, C., Gong, W., Mao, Y., and Ji, C. (2012) Crystal structure of Human ASB9-2 and substrate-recognition of CKB. *Protein J. 31*, 275−284.

(50) Prabhu, N. V., and Sharp, K. A. (2005) Heat capacity in proteins. *Annu. Rev. Phys. Chem. 56*, 521−548.

(51) Robertson, A. D., and Murphy, K. P. (1997) Protein structure and the energetics of protein stability. *Chem. Rev. 97*, 1251−1268.

(52) Sedgwick, S. G., and Smerdon, S. J. (1999) The ankyrin repeat: a diversity of interactions on a common structural framework. *Trends Biochem. Sci. 24*, 311−316.

(53) Mosavi, L. K., Cammett, T. J., Desrosiers, D. C., and Peng, Z. Y. (2004) The ankyrin repeat as molecular architecture for protein recognition. *Protein Sci. 13*, 1435−1448.

(54) Orlicky, S., Tang, X., Neduva, V., Elowe, N., Brown, E. D., Sicheri, F., and Tyers, M. (2010) An allosteric inhibitor of substrate recognition by the SCF(Cdc4) ubiquitin ligase. *Nat. Biotechnol. 28*, 733−737.

(55) Buckley, D. L., Van Molle, I., Gareiss, P. C., Tae, H. S., Michel, J., Noblin, D. J., Jorgensen, W. L., Ciulli, A., and Crews, C. M. (2012) Targeting the von Hippel-Lindau E3 ubiquitin ligase using small molecules to disrupt the VHL/HIF-1alpha interaction. *J. Am. Chem. Soc. 134*, 4465−4468.

(56) Wu, L., Grigoryan, A. V., Li, Y., Hao, B., Pagano, M., and Cardozo, T. J. (2012) Specific small molecule inhibitors of Skp2-mediated p27 degradation. *Chem. Biol. 19*, 1515−1524.